MATHEMATICAL MODELING AND SIMULATION OF RADIAL TEMPERATURE PROFILE OF STRONTIUM BROMIDE LASERS

Snezhana Gocheva-Ilieva

Abstract. *For metal and metal halide vapor lasers excited by high frequency pulsed discharge, the thermal effect mainly caused by the radial temperature distribution is of considerable importance for stable laser operation and improvement of laser output characteristics. A short survey of the obtained analytical and numerical-analytical mathematical models of the temperature profile in a high-powered He-$SrBr_2$ laser is presented. The models are described by the steady-state heat conduction equation with mixed type nonlinear boundary conditions for the arbitrary form of the volume power density. A complete model of radial heat flow between the two tubes is established for precise calculating the inner wall temperature. The models are applied for simulating temperature profiles for newly designed laser. The author's software prototype LasSim is used for carrying out the mathematical models and simulations.*

Keywords: radial heat flow, heat conduction equation, nonlinear boundary conditions, analytic model, metal vapor laser, computer simulation, .NET Framework.4

2010 Mathematics Subject Classification: 80A20, 78A60, 80-04, 81T80

1. Introduction

The application of mathematical models in the spheres of nanotechnology, laser physics, and laser technologies for studying, designing and simulating experiments, as well as for developing new devices, is one of the most powerful modern tools in this high-priority field of science. With the help of mathematical modeling, development time and costs can be reduced along with the need for highly-qualified human labor.

This paper examines a Strontium bromide vapor laser ($SrBr_2$). This laser is one of the latest inventions in the field. Stable laser generation was achieved for the first time in 2002 [1], and in 2006-2009 the laser was significantly improved and patented by the team of the Laboratory of Metal Vapour Lasers at the Institute of Solid State Physics of the Bulgarian Academy of Sciences. One of the important prospects for this laser is connected with its radiation at 6.45 μm, which as shown in [2,3], is the most effective means for soft tissue and bone ablation with minimum thermal damage and pollution during operations. In addition to its medical applications, the $SrBr_2$ laser can be used in lithography, photochemistry, photobiology, atmospheric humidity studies, etc. [4].

An important problem for the stable functioning of metal vapor lasers, and in particular Strontium bromide vapor lasers, is maintaining an optimal temperature mode of the neutral gas in the laser tube. Thermoionizing processes occur when gas temperature increases above a certain level, resulting in a deterioration of the mode composition and the termination of laser generation. It needs to be noted that it is impossible to directly measure the temperature of the neutral gas inside the laser tube because of the high frequency. Only the temperature of the outer wall of the tube under the insulation is measured. The currently existing mathematical models are inaccurate and ineffective since they calculate gas temperature by giving the measured temperature of the outer wall as the temperature of the inner wall of the tube. What is more, the variable radial distribution of volume power density in the active volume is not taken into account, and neither are the structure of the composite walls with its characteristics or external environment conditions. This means that when modeling new devices, where the temperature of the walls is unknown, the temperature within the tube cannot be determined. Models for calculating gas temperature are also an important element of various kinetic models, describing the physical processes within the discharge over periods of time.

These problems have been solved by the analytical and numeric-analytical models we have constructed. This paper surveys some mathematical models of radial temperature distribution in the cross-section of the tube, developed in [5,6], which take into account geometric design, structural element properties, and the qualitative distributions of volume power density. A brief description has been provided of the prototype of the developed software package LasSim [7], part of which is designed to conduct simulations using the models. Some numerical results from the conducted simulations for the laser device [8,9] being recently and continuously developed are presented. They show good correspondence between the experiment and simpler previously-known models.

2. Experimental setup

In this study we are going to examine the high-powered Strontium bromide vapor laser, investigated experimentally in [8,9]. This is a self-heated device. The cross-section of the active volume is given in Figure 1. The total length of the laser tube is 2.30 m, and the length of the active medium (the distance between the electrodes) is $l_a = 0.98\text{m}$. The laser tube is entirely made out of quartz (position (3)), with an additional ceramic tube made out of Al_2O_3, (position (1)) inserted in the active volume. The free space between the two tubes is filled with the buffer gas Helium (position (2)). On the outside the active volume is lined with a heat insulating ZrO_2 coating or with mineral wool (position (4)). The total power consumption of the laser is $Q_{tot} = 2100W$. Taking into account losses (about 35%), the active medium is supplied with Q = 1365 *W* of effective electrical power, or the average volume power density is $q_v = q_0 = 4.55W/cm^3$. Total laser output power is 4 W, with 90% of it at the 6.45μm line [9].

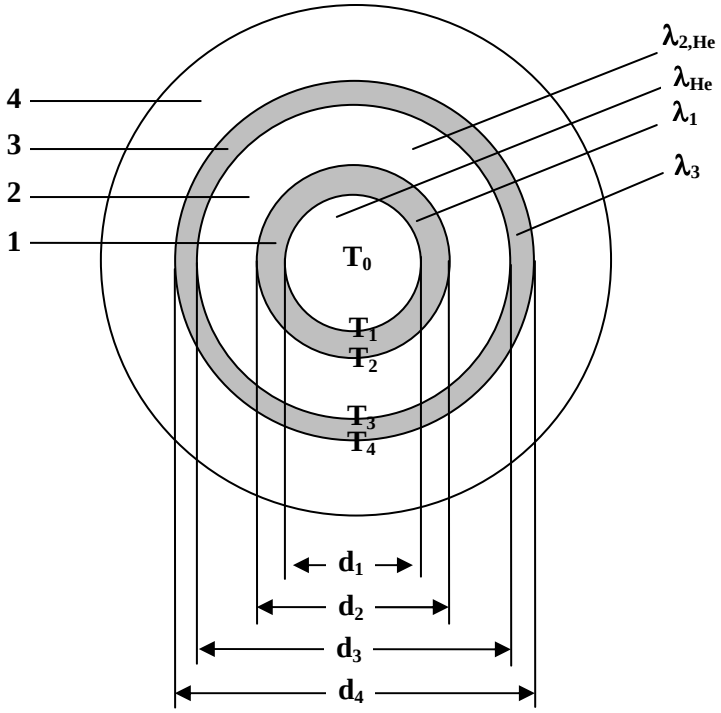

Figure 1. The geometrical design of the cross-section of the laser tube of He-$SrBr_2$ laser: (1) - ceramic (Al_2O_3) tube, (2) – space filled with Helium, (3) - quartz tube and (4) - ZrO_2 insulation. The diameters are as follows: $d_1 = 19.8\,\text{mm}$, $d_2 = 25.5\,\text{mm}$, $d_3 = 40\,\text{mm}$, and $d_4 = 46\,\text{mm}$, $R_1 = d_1 / 2$.

3. Reduced boundary value problem

The models were derived at the following assumptions: (i) the temperature profile is determined in a stationary temperature regime; (ii) in the inter-impulse period the gas temperature does not change significantly; (iii) the total effective electric power supplied to the active volume is transformed into heat. The power transferred to the walls as a result of the discharge radiation and the deactivation of the excited and charged particles is not taken into account; (iv) the thermal radiation of the heated gas in the active volume is ignored.

In stationary operation mode, the gas temperature T_g in the cross-section of the discharge in the inner tube of the laser tube (Figure 1) satisfies the heat conduction equation:

(1) $$\text{div}\left(\lambda_g \text{grad} T_g\right) + q_v = 0,$$

where λ_g is the heat conduction coefficient of the gas, q_v is the volume power density of the internal heat source, and T_g is the unknown temperature of the gas.

Considering the axial and longitudinal symmetry, it can be shown that equation (1) can be reduced to the following one-dimensional equation with respect to the radius *r:*

(2) $$\frac{1}{r}\frac{d}{dr}\left(r\lambda_g\frac{dT_g}{dr}\right)+q_v=0,\quad 0\le r\le R_1,\ R_1=d_1/2.$$

The solution of equation (1), respectively (2), is sought under boundary conditions of the first and second kind:

(3) $$T_g(R_1)=T_1,$$

(4) $$\left.\frac{dT_g}{dr}\right|_{r=0}=0.$$

Commonly, the λ_g is represented in the form $\lambda_g=\lambda_0 T_g^m$, where the constants λ_0, m depend on the kind of the gas. In our case $\lambda_0=0.0027$, $m=0.7057$.

Case I). For $q_v=\text{const}$ the solution of problem (2) - (4) is [10]:

(5) $$T_g(r)=\left[T_1^{m+1}+\frac{q_v(m+1)}{4\lambda_0}\left(R_1^2-r^2\right)\right]^{1/(m+1)},\quad 0\le r\le R_1.$$

Solution (5) has been widely used for gas lasers and metal vapor lasers since 1983 [10] when the unknown value of T_1 is substituted with the measured temperature T_4 of the outer wall or if it is found using unsatisfactory photometrical methods. In the models we have constructed this value is determined using suitable boundary conditions, which have been presented in the next section.

Case II) Improved solution. The right hand side of the equaion (1) has the form

(6) $$q_v = j(x,y)E(x,y),$$

where *j*(*x; y*) is the current density, *E*(*x; y*) is the intensity of the electric field. From $j(x,y)\approx\sigma E$ we have $q_v\approx\sigma E^2$, σ is the field conductivity. From [11] the distribution of field intensity in the cross-section of the tube can be presented by $E(r)=E_0J_0(2.4r/R_1)$, where J_0 is the Bessel function of the first kind of zero order. For q_v in (6) we have $q_v(r)=Q_0\left[J_0(2.4r/R_1)\right]^2$, where the constant $Q_0=2.131q_0$ [6]. The Bessel function J_0 is well-known and represented in a table (see for instance [12]). The expression $\left[J_0(2.4r/R_1)\right]^2$ can be approximated [5] by a polynomial of the third degree as $\left[J_0(x)\right]^2\approx a_1+a_2x+a_3x^2+a_4x^3$, where $x=2.4r/R_1$, $a_1=1.0005$, $a_2=-0.016$, $a_3=-0.5702$ and $a_4=0.1687$. Substituting $B=2.4a_2/R_1$, $C=a_3(2.4/R_1)^2$, $D=a_4(2.4/R_1)^3$, for $q_v(r)$ we find

$q_v(r) = Q_0\left(a_1 + Br + Cr^2 + Dr^3\right)$. It is found in [5] that the problem (2)-(4) has the following explicit solution:

(7) $$T(r) = \left\{ T_1^{m+1} + \frac{(m+1)Q_0}{\lambda_0}\left[\frac{a_1}{4}(R_1^2 - r^2) + \right.\right.$$

$$\left.\left. \frac{B}{9}(R_1^3 - r^3) + \frac{C}{16}(R_1^4 - r^4) + \frac{D}{25}(R_1^5 - r^5) \right] \right\}^{\frac{1}{m+1}}.$$

For practical purposes solution (7) is recommended because of its simplicity.

Case III) General analytical solution. For arbitrary type of volume power density $q_v = q_v(r)$ the solution of the problem (2)-(4) is [6]

(8) $$T_g(r) = \left\{ T_1^{m+1} - \frac{(m+1)}{\lambda_0} \int_{\ln R_1}^{\ln r} \left[\int_{-\infty}^{y} \exp(2t)\, q_v\left(\exp(t)\right) dt \right] dy \right\}^{\frac{1}{m+1}}.$$

Solution (8) may involve numerical integration, depending on the form of $q_v(r)$.

4. Boundary conditions for the radial heat flow

In order to determine the unknown temperature T_1 of the inner ceramic wall, together with equation (2) we take into consideration the distribution of the heat flow along the entire radius of the composite tube given in Figure 1.

We set the following boundary conditions, derived in [6]:

Condition A). The temperature T_4 of the outside wall of the quartz tube under the insulation is known. It can be measured directly. Note that the maximum temperature for heating the quartz is 1200 W.

Condition B). Temperature T_3 of the inner wall of the quartz tube (in cylindrical configuration) is [5,6]:

(9) $$T_3 = T_4 + \frac{q_l \ln(d_4/d_3)}{2\pi\lambda_3},$$

where λ_3 is the thermal conductivity of the type of quartz used.

Condition C). The space between the two tubes (Fig. 1-(2)), is filled with Helium. The condition is:

(10) $$Q = \varepsilon_{eff} c \left[\left(\frac{T_2}{100}\right)^4 - \left(\frac{T_3}{100}\right)^4 \right] S_2 + \frac{2\pi\lambda_{2,He} l_a}{\ln\left(d_3/d_2\right)}\left(T_2 - T_3\right) + \frac{2\pi\lambda_{eff} l_a}{\ln\left(d_3/d_2\right)}\left(T_2 - T_3\right)$$

where $\lambda_{2,He}$ is the thermal conductivity of the helium between the tubes. Further we will consider (10) as a sum of three respective summands

(11) $$Q = Q_1 + Q_2 + Q_3.$$

In [6] the condition (10) was obtained in the form

$$Q=\varepsilon_{eff}\,c\left[\left(\frac{T_2}{100}\right)^4-\left(\frac{T_3}{100}\right)^4\right]S_2+\frac{2\pi l_a\left(T_2-T_3\right)}{\ln(d_3/d_2)}\lambda_0\left(0.5\left(T_2+T_3\right)\right)^m$$

$$+\frac{2\pi l_a\left(T_2-T_3\right)}{\ln(d_3/d_2)}\lambda_0\left(0.5\left(T_2+T_3\right)\right)^m\times 0.386\left(\frac{\mathrm{Pr}}{0.861+\mathrm{Pr}}\right)^{1/4} \tag{12}$$

$$\times\frac{\ln(d_3/d_2)}{\delta^{3/4}\left(d_2^{-4/5}+d_3^{-4/5}\right)^{5/4}}\left(\frac{\dfrac{g}{0.5\left(T_2+T_3\right)}\left(T_2-T_3\right)\delta^3}{\left(\upsilon_0\left[0.5\left(T_2+T_3\right)\right]^{a+1}\right)^2}\mathrm{Pr}\right)^{1/4}$$

where

$$\varepsilon_{eff}=\left(\frac{1-\varepsilon_1}{\varepsilon_1}.\frac{S_2}{S_3}+\frac{1}{F_{23}}+\frac{1-\varepsilon_2}{\varepsilon_2}\right)^{-1},\ \delta=\frac{d_3-d_2}{2}. \tag{13}$$

Condition D). The equation for the inner wall temperature T_1 of the ceramic tube is [5,6]:

$$T_1=T_2+\frac{q_l\ln(d_2/d_1)}{2\pi\lambda_1}, \tag{14}$$

where λ_1 is the thermal conductivity of the type of ceramic material used.

The notations used in equations (9)-(14) are as follows (see in details [5,6]): The quantity Q is the heat flow equal to the effective input electric power, regarding the model assumptions, ε_{eff} is an effective radiation coefficient, taking into account the multiplex reflections in the space between the two tubes (Fig.1 – (2)), F_{23}=0.8, $S_2=\pi l_a d_2$, $S_3=\pi l_a d_3$, g is the gravitational acceleration, Prandtl number $\mathrm{Pr}=0.67$, $\lambda_1=2.08W/(mK)$, $\lambda_3=1.96W/(mK)$, $\varepsilon_1=0.52$, $\varepsilon_2=0.72$, $a=0.6953$.

Boundary conditions (9) and (14) take into account the process of heat transfer through heat conduction. In boundary condition (10)-(11) the first summand Q_1 represents the Stefan-Boltzmann law and describes the heat exchange by radiation of the ceramic tube in an enclosed space (Fig.1 –(2)), Q_2 stands for Newton-Richman's law and describes the process of heat conduction. The third summand Q_3 in (10)-(11) describes the free convection in an enclosed space (Fig.1–(2)). In this way, boundary conditions (10) take into account all possible processes of heat transfer: radiation, heat conduction and free convection.

When the temperature of the quartz tube T_4 is known (insulated), the temperature T_3 is determined using (9). In equation (12) the unknown is the temperature T_2. With respect to T_2 equation (12) is nonlinear and does not provide an exact algebraic solution. The unknown temperature T_2 could be found by

numerically solving (12). After calculating T_2, through (14) we find T_1. In this way we obtain the reduced boundary value problem: equation (2) with a known temperature T_1 and boundary conditions (3) and (4). Depending on the type of volume power density q_v this problem has solutions (5), (7) or (8).

5. LasSim prototype and application of the model for computer simulations

A working prototype of the software package LasSim was developed in order to conduct computer simulations of the physical processes and to evaluate various characteristics of metal vapor lasers. The package includes 15 models, two of which are relevant to the Strontium bromide vapor laser at hand.

The prototype LasSim [8] is an Windows application designed on .NET Framework 4, WPF and C# technologies, which gives the opportunities for installing and managing different model simulation processes. Modules are created by using Microsoft Visual Studio Fortran. Any simulation module can perform given model simulation, by using its corresponding input files and generates the output results files. Post-processing and simple text and graphical representation of the results are realized.

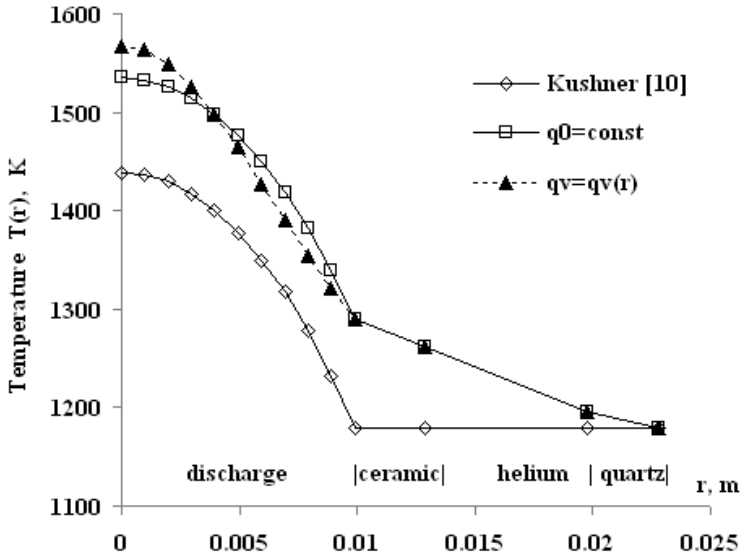

Figure 2. Distribution of the radial temperature profile in a half cross-section of the laser tube, found by the tree different models at total input electric power $Q_{tot} = 2100W$.

As an application of the models we first carry out the simulations of the radial heat flow along the composite wall at supplied electric power wich is the real quantity in laser [9]. By the LasSim we obtain the results, shown in Figure 2. We

observe a difference of about 100K to 130 K between the maximum gas temperature in the center of the tube ($r = 0$) between the Kushner method [10] and the accurately applied solution (5) at $q_0 = \text{const}$ and (7) with conditions (9), (12-13). This illustrates the quality of the constructed models.

As a second example in Figure 3 there are presented the some results from the simulations of the gas temperature profile for the same $SrBr_2$ laser [9], where the solution (7) with conditions (9), (12-13) is applied for different input electric power $Q_{tot} = 2100W, 2200W$ and $2300W$. It was assumed that the effective power $Q = 0.65 Q_{tot}$. It is observed an increase of the maximum temperature within 3-4%. This way we can expect an optimal operating temperature in the center of the laser tube around 1580 K. This is in good agreement with the experimental evaluation.

Other type of simulations can be used to investigate more than 15 laser parameters, including diameters of the tube, thermal conductivities of the materials, outside wall temperature, possible inserts in the tube, gas pressure, gas compounds and more.

Figure 4 shows the output text interface of the prototype Lassim with the results, illustrated in Figure 3 for $Q_{tot} = 2300W$ (or $Q = 1495W$).

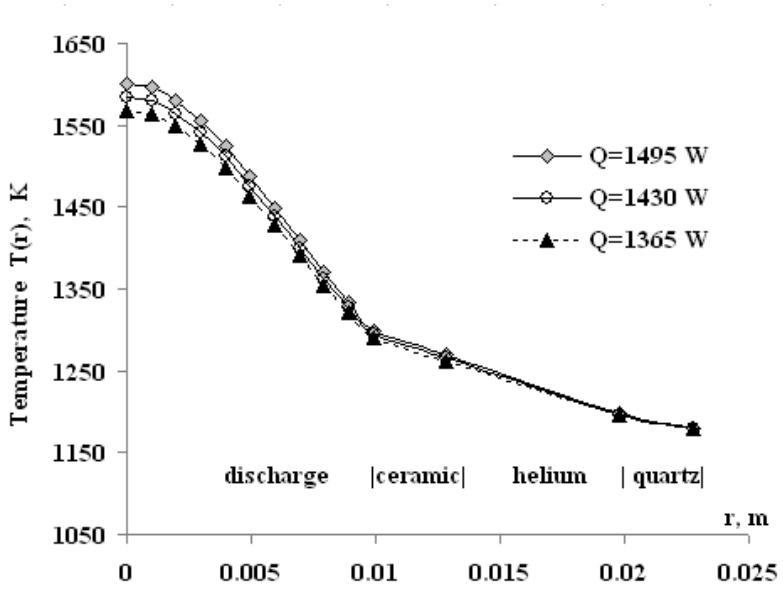

Figure 3. Temperature profile in a half cross-section of the laser tube for different effective input electric power Q.

6. Conclusion

There are presented some of the recently obtained results in construction of mathematical models for evaluation of the radial heat flow in strontium bromide laser. The models are applied for computer simulations of the temperature profile

via the software prototype LasSim. The comparison between the existing and the presented models shows a strong advantage of the new models. The obtained results are in good agreement with the experiment.

This work is supported by Plovdiv University NPD, Project RS-M-13.

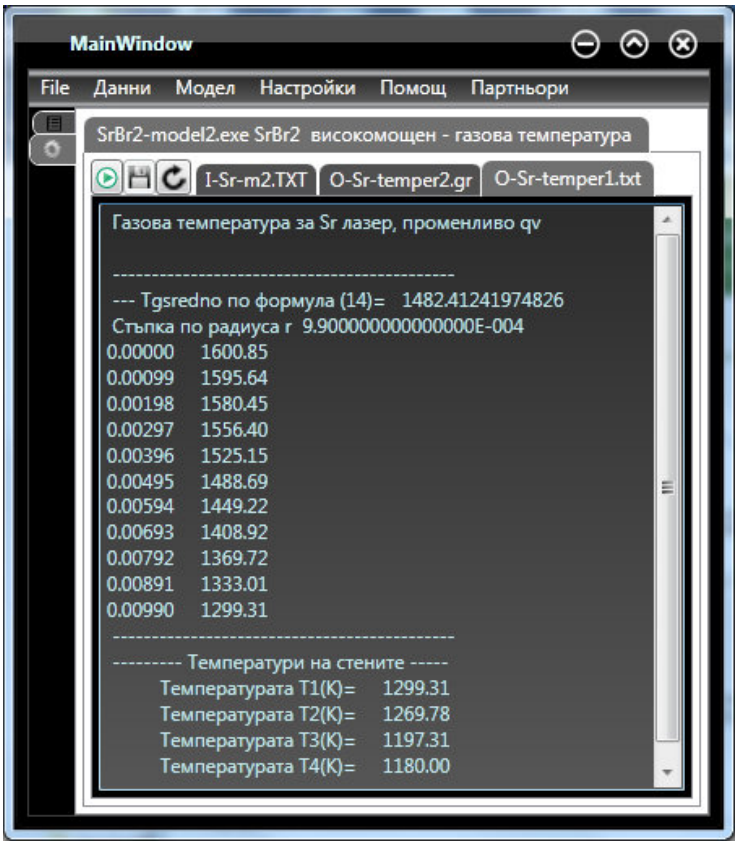

Figure 4. Output text file of the LasSim prototype.

References

[1] B.L. Pan, Z.X. Yao, G. Chen, A discharge –excited SrBr2 vapour laser, Chin. Phys. Lett., 19, no. 7 (2002) 941-943.

[2] G. M. Peavy, L. Reinisch, G. T. Rayne, and V. Venugopalan, Comparison of cortical bone ablations by using infrared laser wavelength 2.9 to 9.2 µm, Laser in Surgery & Medicine, 25 (1999) 421-434.

[3] J. M. Auerhammer, R. Walker, A. F. G. van der Meer, B. Jean, Dynamic behavior of photoablation products of corneal tissue in the mid-IR: a study with FELIX, Applied Physics B: Lasers and Optics, 68 (1999) 111-119.

[4] C. E. Webb, J.D.C. Jones, Handbook of Laser Technology and Applications, Vol. 3: Applications, Institute of Physics Publishing, Taylor & Francis, Bristol and Philadelphia, 2003.
[5] I.P. Iliev, S.G. Gocheva-Ilieva, K.A. Temelkov, N.K. Vuchkov, N.V. Sabotinov, Analytical model of temperature profile for a He-SrBr2 laser, J Optoelectron Adv Mater, 11 (11), (2009) 1735 – 1742.
[6] I.P. Iliev, S.G. Gocheva-Ilieva, K.A. Temelkov, N.K. Vuchkov, N.V. Sabotinov, An improved radial temperature model of a high-powered He-SrBr2 laser, J Optics and Laser technology, Elsevier, 43, (2011), 642-647.
[7] S.G. Gocheva-Ilieva, C.P. Kulin, Development of LasSim software prototype for simulating physical characteristics of laser devices, Scientific Works of Plovdiv University, 37- Mathematics (in print).
[8] K. A. Temelkov, N. K. Vuchkov, B. L. Pan, N. V. Sabotinov, B. Ivanov, L. Lyutov, J. of Physics D: Applied Physics, 39 (2006) 3769-3772.
[9] K. A. Temelkov, N. K. Vuchkov, B. Mao, E. P. Atanassov, L. Lyutov, N. V. Sabotinov, IEEE Journal of Quantum Electronics, 45 (2009) 278-281.
[10] M.J. Kushner, B.E. Warner, Large-bore copper-vapor lasers: Kinetics and scaling issues, J. Appl. Phys. 54 (1983) 2970-2982.
[11] P. Blau, Impedance matching and electric field penetration in metal vapour lasers, in Pulsed metal vapor lasers – physics and emerging applications in industry, medicine and science, eds: C.E. Little and N.V. Sabotinov, Kluwer Academic Publishers, Dordreht, 1996, 215-220.
[12] M. Abramowitz, I. Stegun, Handbook of Mathematical Functions with Formulas, Graphs, and Mathematical Tables, nine ed., Dover Publications, New York, 1964.
[13] .NET Framework Developer Center http://msdn.microsoft.com/en-us/netframework/default.aspx

Snezhana Gocheva-Ilieva
Faculty of Mathematics and Informatics
University of Plovdiv
236 Bulgaria Blvd.
4003 Plovdiv, Bulgaria
e-mail: snow@uni-plovdiv.bg